FOA (first-order-analysis) model of an expandable lattice structure for vehicle crash energy absorption of an inflatable morphing body

Dong Wook Lee[1], Zheng-Dong Ma*[2] and Noboru Kikuchi[2]

[1]*R&D Center, Samsung Techwin, Seongnam-Si, Kyunggi-Do 463-400, Korea*
[2]*Department of Mechanical Engineering, University of Michigan, Ann Arbor, MI, 48109, USA*

Abstract. A concept of crash energy absorbing (CEA) lattice structure for an inflatable morphing vehicle body (Lee *et al.* 2008) has been investigated as a method of providing rigidity and energy absorption capability during a vehicular collision (Lee *et al.* 2007). A modified analytical model for the CEA lattice structure design is described in this paper. The modification of the analytic model was made with a stiffness approach for the elastic region and updated plastic limit analysis with a pure plastic bending deformation concept and amended elongation factors for the plastic region. The proposed CEA structure is composed of a morphing lattice structure with movable thin-walled members for morphing purposes, members that will be locked in designated positions either before or during the crash. What will be described here is how to model the CEA structure analytically based on the energy absorbed by the CEA structure.

Keywords: lattice structure; crashworthiness; crash energy absorption; inflatable morphing body.

1. Introduction

Previous research on crashworthiness designs of automotive bodies usually focused on the tube structure or material design, which includes cross section and shape (Kim and Wierzbicki 2001, Han and Yamazaki 2003, Suh *et al.* 2002, Avalle *et al.* 2002, Alghamdi 2001), honeycomb sandwich structures (Yasui 2000, Aktay *et al.* 2005), and alternative materials (Deb *et al.* 2004). The current cars, unfortunately, contain fundamental handicaps including fixed front end structures and limited crumple zones with the fatality rate dramatically increased in high speed impacts. In order to design a successful lightweight vehicle and significantly improve the crash performance of current cars, technology development is still needed. Therefore, Lee *et al.* (2008) proposed a new concept called "inflatable bumper." The expandable lattice structure (ELS) presented in this paper is one of components of the inflatable bumper. Fig. 1 illustrates an example prototype of such ELS.

In this research, analytic modeling of the expendable lattice structure is conducted. This structure is used to absorb the crash energy of colliding cars that have inflatable bumpers. As illustrated in

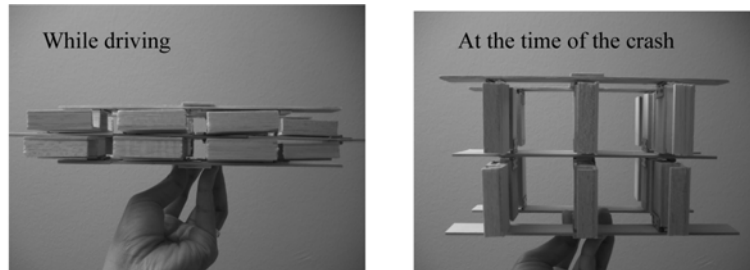---

*Corresponding author, Ph.D., E-mail: mazd@umich.edu

Fig. 1 Prototype of expandable lattice structure for crashworthiness

Fig. 1, the ELS is folded while driving, and is expanded and locked during the crash in order to absorb the crash energy. It is assumed that a sophisticated sensor and radar system is available to detect an impending collision. Lee *et al.* (2007) have developed an analytic model for the ELS based on strain energy using a stress and strain curve, Young's modulus, as well as a reduced modulus for elastic regions and a plastic limit analysis for plastic regions. In this paper, an advanced model for the ELS was developed based on a stiffness approach and a modified plastic limit analysis, which results in much improved prediction accuracy.

Usually in mechanical or civil engineering, a lattice structure utilizes beam elements or bar elements, analytic modeling of such lattice structures has been done for strength and stiffness (Pedersen and Nielsen 2003, Sedaghati *et al.* 2001, Kawamura *et al.* 2002) and for frequency constraints (Lingyun *et al.* 2005) to avoid resonance. Pedersen (2004) has also studied crashworthiness design of a frame structure, for a passive (fixed) structure.

The thin-walled member of the proposed lattice structure is composed of plates. Therefore analytic modeling should be performed for the plates instead of for beams or bars. It is assumed that the pressure is evenly distributed between the upper and lower plates, that every thin-walled member in the lattice structure is under the same boundary and loading conditions, and that every thin-walled member has the same shape, size, and material properties. To calculate the crash energy absorbed in the lattice structure, the deformation region can be separated into a pre-global buckling region where a local buckling can occur and a post-global buckling region where plastic joints are
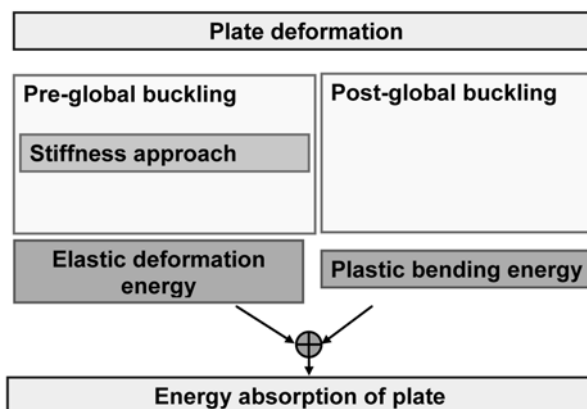

Fig. 2 Pre-global buckling region and post-global buckling region in plate crush behavior
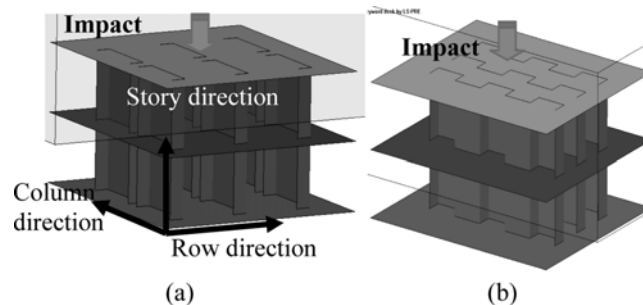
Fig. 3 Lattice structure with the *U* shape of (a) a thin-walled member and (b) rectangular jagged member

formed (see Fig. 2). For the pre-global buckling region, the elastic deformation energy is superposed of elastic deformation energy of individual thin-walled member elements in parallel and series based on the stiffness of the single plate theory. For the post-global buckling region, this research applies the theory of plastic limit analysis that is updated with pure plastic bending deformation and amended elongation factors for plastic region from the previous paper (Lee *et al.* 2007) to an absorbed energy in the lattice structure. In the previous paper, the plastic bending deformation included an elastic bending deformation and the elongation factors were only based on the width of cross section of thin-walled member. Final energy absorption by the lattice structure can be obtained by summation of the absorbed energies in the pre-global buckling region and the post-global buckling region.

Two kinds of elements for thin-walled members in the lattice structure have been considered in this research. One is the *U* shape of the thin-walled member (see Fig. 3(a)) and the other is the rectangular jagged thin-walled member (see Fig. 3(b)). Analytic modeling in this paper is based on the *U* shape of the thin-walled member. The analytic model developed can be easily applied to the rectangular jagged member with minor changes. For the material properties, it is assumed to be elastic-perfect plastic material.

Many materials are strain rate sensitive, and the yield stress increases as the strain rate increases. In this research, the strain rate effect has been neglected.

2. Absorbed energy in the pre-global buckling region based on the stiffness approach

In this section, the approach for energy absorption in the pre-global buckling region is investigated based on the stiffness theory (Malen and Kikuchi 2006). First of all, the analytic model for energy absorbed in a single plate in the lattice structure is investigated and then the developed analytic model is expanded to the whole lattice structure, including multiple plates based on superposition theory of elastic elements connected serially and in parallel.

2.1 Stiffness of a single plate in the lattice structure

During a crash, a plate in the lattice structure will undergo buckling, possibly locally or globally. In this subsection, we investigate an approach which is based on the stiffness derived from the plate

buckling theory that is used to estimate the absorbed energy in a single plate for the pre-global buckling region. The plate of the lattice structure will undergo a local buckling within the plate before global buckling takes place during the crash. A plate can still carry an increased load before global buckling occurs, even if it goes through local buckling under the axial load condition (see Fig. 4). Therefore, we can calculate the energy absorbed in a plate before global buckling occurs based on elastic stiffness.

   Expressions for estimating the stiffness, K_1 and K_2, (see Fig. 4) of a single plate (see Fig. 5) in the lattice structure before and after local buckling occurs, are developed. The developed expression can then be applied to every single plate in this lattice structure without any modifications because it is assumed that every plate in the lattice structure have the same shape, size, and material properties,
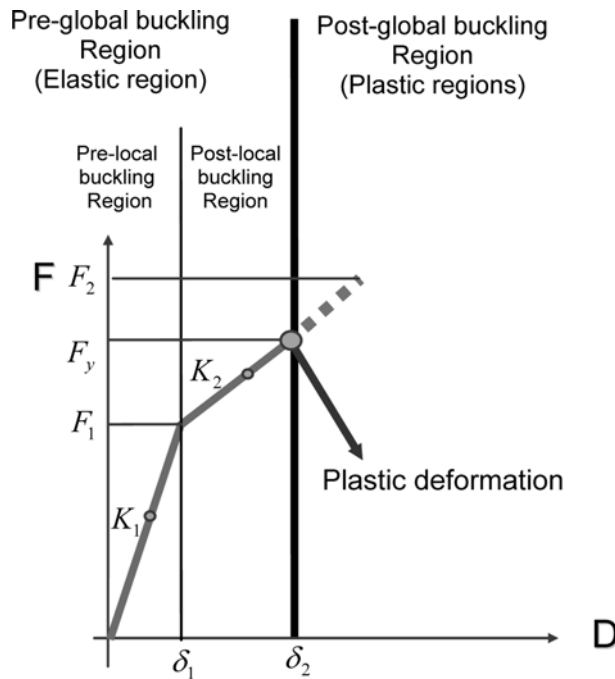

Fig. 4 Elastic region and plastic region in plate crush behavior based on plate buckling theory
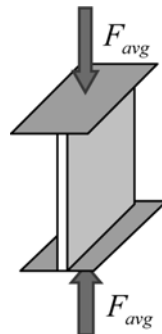

Fig. 5 Load path of a single plate in lattice structure

and the structure is constructed by repeating the same plate.

Fig. 5 shows the load path of a single plate in the lattice structure. The U shape of the thin-walled member (see Fig. 3(a) and Fig. 9) will be considered in Section 2.2. In Fig. 5, the upper plate and lower plate are assumed to be rigid. Actually, the load in the lateral direction, from the connection of the upper plate and lower plate, has an insignificant influence on the axial and bending deformation of the plate.

Work done by the external force (F_{avg}) is the same as strain energy stored in the structure, which is

$$\frac{1}{2}F_{avg}\Delta = U \tag{1}$$

where displacement (Δ) can be expressed as a force divided by a stiffness coefficient K

$$\Delta = \frac{F_{avg}}{K} \tag{2}$$

Therefore, stiffness of a single plate can be expressed from Eqs. (1) and (2) as

$$K = (F_{avg})^2/(2U) \tag{3}$$

Considering only the longitudinal stress, the strain energy stored in a single plate (Hibbeler 2005) can be given simply as

$$U = \int \sigma d\varepsilon dV = \int \frac{\sigma^2}{2E}dV = \frac{\sigma^2 abt}{2E} \tag{4}$$

where E, σ, a, b, and t denote Young's modulus of plate, axial stress of plate, width of plate, length of plate, and thickness of plate, respectively. It is necessary to find the stress of a plate in Eq. (4) in order to determine the absorbed strain energy U. This stress can be considered in two cases: before local buckling and after local buckling. First, consider the stiffness K_1 of Fig. 4. The stress of plate before local buckling is expressed by

$$\sigma = F_{avg}/(at) \tag{5}$$

From Eqs. (4) and (5), the strain energy stored by the plate is

$$U = \frac{\sigma^2 abt}{2E} = \frac{F_{avg}^2 b}{2Eat} \tag{6}$$

Therefore, the stiffness of the plate before local buckling can be expressed as

$$K_1 = \frac{Eat}{b} \tag{7}$$

Consider the stress and stiffness of the plate after local buckling occurs, but before global buckling takes place. The stress on the compressive plate can be written on the basis of the effective width theory (Malen and Kikuchi 2006) as

$$\sigma = F_{avg}/(a_e t) \tag{8}$$

where a_e denotes an effective width,

$$a_e = \frac{a}{2}\left(1 + \frac{\sigma_{cr}}{\sigma}\right)$$

$$\sigma = \begin{cases} \sigma_{cr} \text{ at the point where buckling begins} \\ \sigma_y \text{ at the point where failure begins} \end{cases}$$

σ_{cr}: critical compressive plate (local) buckling stress
σ_y: yield stress

The critical compressive plate buckling stress can be written as (Yu 2000)

$$\sigma_{cr} = k\frac{E\pi^2}{12(1-\mu^2)(a/t)^2} \tag{9}$$

where k, E, μ, a and t denote the constant for the boundary condition of a single plate, Young's modulus, Poisson's ratio, the width of a single plate, and the thickness of a single plate, respectively. So, the strain energy stored in the plate from Eq. (4) yields

$$U = \frac{\sigma^2 a_e bt}{2E} \tag{10}$$

The average effective thickness during the local buckling can be assumed to be

$$a_e = \frac{a}{2}\left(1 + \frac{2\sigma_{Cr}}{\sigma_{Cr} + \sigma_y}\right) \tag{11}$$

Therefore, the average stiffness of the plate in the time between local buckling and global buckling can be given by

$$K_2 = \frac{a_e tE}{b} = a\left(1 + \frac{2\sigma_{cr}}{\sigma_{cr} + \sigma_y}\right)Et/(2b) \tag{12}$$

Fig. 6 shows the comparison of stiffness of a single plate under compression obtained by our measurements and those of Rhodes (2001). As can be seen, the stiffness (K_1 and K_2) before buckling and after buckling is in a similar format.

This work	Rhodes's work (Rhodes 2001)

$$K_1 = \frac{Eat}{b} \qquad\qquad K_1 = \frac{Eat}{b}$$

$$K_2 = \frac{aEt}{b}\times\left(\frac{1}{2} + \frac{\sigma_{cr}}{\sigma_{cr} + \sigma_y}\right) \qquad K_2 = \frac{aEt}{b}\times(1-K_l)$$

$$* (1-K_l) = 18/35$$
$$\textit{for unloaded edges fixed} - \textit{fixed}$$
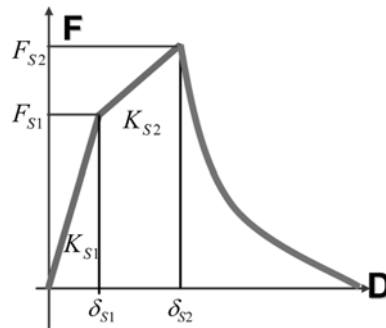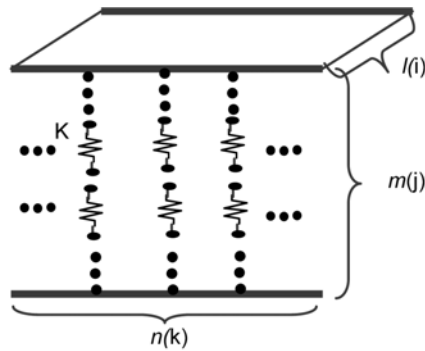
Fig. 6 Stiffness of a single plate

Fig. 7 F-D curve of lattice structure

$$K_{S1\,or\,S2} = \sum_{i=1}^{l}\sum_{k=1}^{n}\left(1\Big/\sum_{j=1}^{m}\frac{1}{K_{ijk}}\right) \;\Rightarrow\; K_{S1\,or\,S2} = K_p \times (n)(l)/(m)$$

K_p: spring constant of a single plate

l: # of columns m: # of stories n: # of rows

Fig. 8 Serial and parallel combination of plates in lattice structure

2.2 Stiffness of the lattice structure

The stiffness of a single plate has been obtained in Section 2.1. To obtain the stiffness (represented by K_{S1} and K_{S2} in the F-D curve in Fig. 7) of a lattice structure composed of multiple identical plates, plates are superimposed using the serial and parallel theories of connected elastic elements represented by the springs (see Fig. 8).

Assume the element in the truss structure to be the U shape of a thin-walled member as in Fig. 3. Then the U section can be isolated with a given boundary condition, as in Fig. 9. Therefore the critical stress (Eq. (9)) for each plate in the U section element can be obtained separately (Schafer 2002). So, the stiffness of the plate in the element will be calculated independently.

For the connection of two adjacent plates in Fig. 9, if the thicknesses of two plates are different (that is, one is thicker and the other one is thinner), the boundary condition for the connection can be defined as fixed. However, if the thicknesses of two plates are the same, the boundary condition
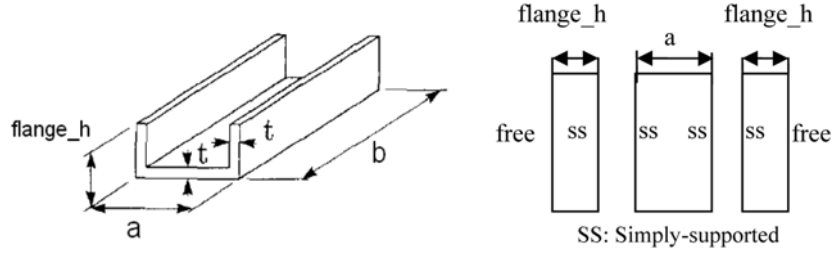
Fig. 9 Element to be repeated in lattice structure and plate edge condition for buckling coefficient *k*

for the joint can be considered to be simply-supported (Malen and Kikuchi 2006). In our lattice structure, the thicknesses of all of the plates are assumed to be the same, so the plate edges can be modeled as simply-supported as shown in Fig. 9.

Considering serial and parallel combination of Fig. 8 and the *U*-shape section of Fig. 9 with Eqs. (7) and (12) results in

$$K_{S1} = \frac{n_{row}n_{column}}{n_{story}}\left(\frac{Eat + 2 \cdot E \cdot flange\_h \cdot t}{b}\right) \tag{13-1}$$

$$K_{S2} = \frac{n_{row}n_{column}}{n_{story}}\left(\frac{\left(at\left(1+\frac{2\sigma_{cr\_web}}{\sigma_{cr\_web}+\sigma_y}\right)+2 \cdot flange\_h \cdot t \cdot \left(1+\frac{2\sigma_{cr\_flange}}{\sigma_{cr\_flange}+\sigma_y}\right)\right)E}{(2b)}\right) \tag{13-2}$$

where K_{S1} and K_{S2} are extensions of Eqs. (7) and (12), respectively. σ_{cr_web} and σ_{cr_flange} are the critical stress for the web part and the critical stress for the flange part, and *n_row*, *n_column*, and *n_story* are the number of elements in the direction of the row, the number of elements in the direction of the column, and the number of elements in the direction of height, respectively (see Fig. 3).

2.3 Critical forces, critical displacement, and absorbed energy in lattice structure

The total force on a *U*-shaped element can be obtained areas

$$F = \sigma_{web}A_{web} + 2\sigma_{flange}A_{flange} \tag{14}$$

According to the superposition theory, the total force of lattice structure is affected only by springs connected in parallel. The stress at the point where local buckling begins is a critical compressive plate buckling stress (see Eq. (9)). Therefore, the critical force at the point where local buckling begins (F_{S1}) can be expressed as

$$F_{S1} = n_{row}n_{column}\left(k_{web}\frac{E\pi^2}{12(1-\mu^2)(a/t)^2}at + 2k_{flange}\frac{E\pi^2}{12(1-\mu^2)(flange\_h/t)^2}flange\_h \cdot t\right) \tag{15}$$

At the point where failure (global buckling) begins

$$A = a_e t, \quad \sigma = \sigma_y, \quad \text{where} \quad a_e = \frac{a}{2}\left(1+\frac{\sigma_{cr}}{\sigma_y}\right) \tag{16}$$

And the force for one element is

$$F = \sigma_{y\_web}(a_e t)_{web} + 2\sigma_{y\_flange}(a_e t)_{flange} \tag{17}$$

So, the critical force at the point where global buckling begins (F_{S2}) can be expressed as

$$F_{S2} = \sigma_Y n_{row} n_{column} t \left(\frac{a}{2} \left(1 + \frac{k_{web}\dfrac{E\pi^2}{12(1-\mu^2)(a/t)^2}}{\sigma_Y} \right) + flange\_h \left(1 + \frac{k_{flange}\dfrac{E\pi^2}{12(1-\mu^2)(flange\_h/t)^2}}{\sigma_Y} \right) \right) \tag{18}$$

And, the critical displacements under the critical forces become

$$\delta_{S1} = \frac{F_{S1}}{K_{S1}} \qquad \delta_{S2} = \frac{F_{S1}}{K_{S1}} + \frac{F_{S2}-F_{S1}}{K_{S2}} \tag{19}$$

Using the above equations, the absorbed energy of a lattice structure can be obtained as

$$U_{pre} = \frac{1}{2}K_{S1}\delta_{S1}^2 + F_{S1}(\delta_{S2}-\delta_{S1}) + \frac{1}{2}K_{S2}(\delta_{S2}-\delta_{S1})^2 \tag{20}$$

3. Absorbed energy in the post-global buckling region

In this section, the energy absorbed in the post-global buckling region is investigated. In the post-global buckling region, the plate will be deformed and some part of the plate will go through global plastic bending as shown in Fig. 10. The energy absorbed in post buckling will be the same as the plastic bending energy. To obtain the plastic bending energy, the plastic limit analysis can be applied.

The energy absorbed by the plastic deformation of one element can be given by

$$U^1_{post} = M_p \times \theta_{final} \tag{21}$$

where M_p means a full plastic bending moment and θ_{final} means an average distortion angle in the final position.

To obtain the value of Eq. (21), it is necessary to know the full plastic bending moment and the amount of distortion of the elements in plastic bending. Consider the full plastic bending moment. If
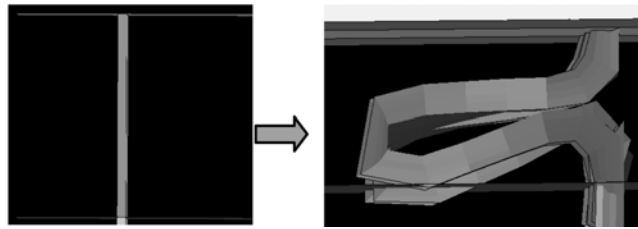

Fig. 10 Deformation of a plate

it is assumed that the plate has a rectangle cross section, he full plastic bending moment (Crandall *et al.* 1978) can be expressed by

$$M_p = \frac{3}{2}M_y = \frac{3}{2}\frac{at^2}{6}\sigma_y = \frac{at^2}{4}\sigma_y \tag{23}$$

where M_y, expressed by $(at^2/6)\sigma_y$ (Crandall *et al.* 1978), denotes a bending moment that corresponds to the onset of yielding in the plate. σ_y, a, and t are yield stress, the width of a plate, and the thickness of a plate, respectively. For the elements in the lattice structure (Fig. 9), the full plastic bending moment can be modified to

$$M_p = \frac{a_{pe}t^2}{4}\sigma_y \tag{23}$$

where a_{pe} means an effective width for plastic moments determined by the function of the width of web, the height of flange, the thickness of plate, and the extra elongation. It can be expressed by

$$a_{pe} = a + 2 \times flange\_h + 2 \times (\alpha_{lattice} \times a/t + \beta_{lattice} \times flange\_h/t) \tag{24}$$

where $\alpha_{lattice}$ and $\beta_{lattice}$ are elongation factors for plastic bending (see Fig. 11), the value of which can be determined by a numerical test. As shown in Fig. 11, after plastic bending, the total width for the element will be increased by some amount. In this research, it can then be assumed that an elongated length is a function of flange height of a plate, the width of a plate, and the thickness of plate like $\alpha_{lattice} \times a/t$ and $\beta_{lattice} \times flange\_h/t$.

Now, consider the amount of distortion of the elements. To find the analytic expression for the amount of distortion, the shape of deformation has been assumed to be a circle or any other polygon that has one loop and two hinges like Fig. 12. It is necessary to know the total deformation angle for the loop and the hinges around the polygon that is modeled.

The deformation angle (exterior angle) for one polygon (loop) that has n sides will be given as the constant
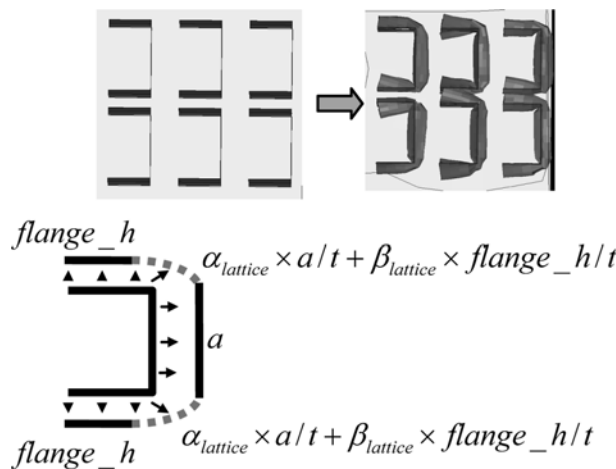

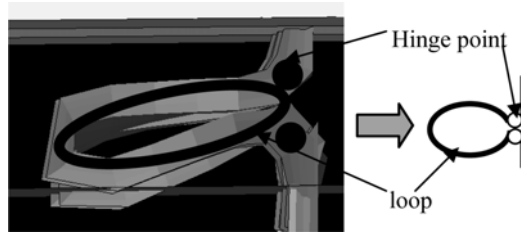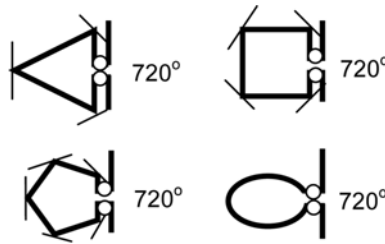Fig. 11 The cross section shape of plates before and after buckling

Fig. 12 The shape of the deformation of a plate (one loop and two hinges)

Two hinges and one loop (polygon)

Fig. 13 Deformation angles of some polygons

$$\left(\pi - \frac{\pi(n-2)}{n} \right) \times n = 2\pi \tag{25}$$

Therefore, it can be considered that the deformation angle in any polygon is always 2π (see Fig. 13). So, regardless of loop shape, the loop can be assigned 2π for its deformation angle, and the hinge can be assigned π for its deformation angle. Then the total deformation angle for elements with one loop and two hinges will be

$$\left(\pi - \frac{\pi(n-2)}{n} \right) \times n + 2\pi = 4\pi \tag{26}$$

2π for the loop shape and π for the hinge are not all associated with the plastic bending deformation, some of them are associated with the elastic bending. This 4π includes a portion of elastic bending deformation that should be not considered. Fig. 14 shows a moment-curvature relation for the bending on the condition that the material is elastic-perfect plastic (Crandall *et al.*
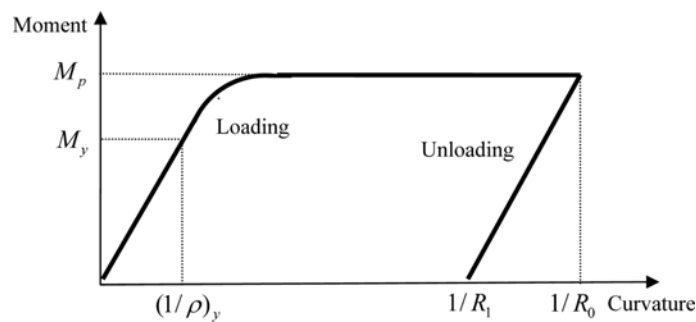

Fig. 14 Moment-curvature relation for loading and unloading of the bending moment
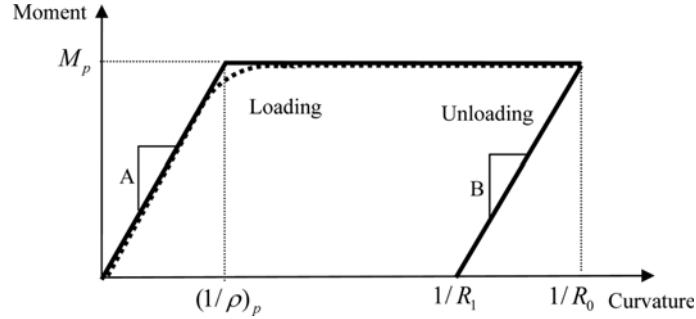
Fig. 15 Simplified moment-curvature relation for loading and unloading of the bending moment

1978). The curve is simplified at Fig. 15 from which the portion of elastic bending deformation can be easily found.

The deformation angle for the elastic bending part will be determined by the curvature, $(1/\rho)_p$ of Fig. 15. The curvature, $(1/\rho)_p$, can be expressed by $1/R_0 - 1/R_1$ because slope A and the slope B are equal. Crandall *et al.* (1978) found the value

$$1/R_0 - 1/R_1 = \frac{3\sigma_y}{Et} \tag{27}$$

So, the corresponding elastic deformation angle can be determined by multiplying Eq. (27) by the length of the arc associated with the elastic deformation angle, which can be expressed simply by *b/(number of hinges and loops)*

Therefore, the elastic deformation angle will be

$$\textit{The elastic deformatio n angle} = \frac{3\sigma_y}{Et} \times \frac{b}{\textit{number of hinges and loops}} \tag{28}$$

The pure plastic deformation angle can be obtained by subtraction of Eq. (28) from Eq. (26).

$$\textit{The plastic deformation angle} = \left(4\pi - 3 \times \frac{3\sigma_y}{Et} \times \frac{b}{3}\right) \tag{29}$$

The deformation angle of an element depends on the number of loops and the number of hinges. In this research, those numbers are determined by a simulation using LS-DYNA. For a *U* shape of a thin-walled member (see Fig. 3), one loop and two hinges are appropriate for almost all cases.

The resulting equation of (21) for the energy absorbed in the post-global buckling region by one element will be

$$U^1_{post} = \frac{(a + 2 \times flange\_h + 2 \times (\alpha_{lattice} \times a/t + \beta_{lattice} \times flange\_h/t))t^2}{4} \sigma_y \times \left(4\pi - 3 \times \frac{3\sigma_y}{Et} \times \frac{b}{3}\right) \tag{30}$$

So, the total strain energy stored in the lattice structure will be the sum of individual plastic bending energies in each element of the lattice structure. That is

$$U_{post} = \sum_1^{n\_row} \sum_1^{n\_column} \sum_1^{n\_story} U^1_{post} = U^1_{post} \times n\_row \times n\_column \times n\_story \tag{31}$$

Finally, the energy absorbed by the lattice structure during elastic and plastic deformation can be described as

$$U_{lattice} = U_{pre}(\text{Eq.20}) + U_{post}(\text{Eq.31}) \tag{32}$$

4. Validation of the analytic model of a crash energy absorption structure using LS-DYNA

The developed analytic model has been verified simply by using LS-DYNA. For the lattice structure crash simulation, the impact mass is 1962 kg and the speed of the mass is 13.4 m/s. The material used in this test is steel that is assumed to be elastic-perfect plastic. The U shape of the thin-walled member (see Fig. 16) was applied to this test.

Fig. 17 and Table 1 demonstrate the total absorbed energy and show the comparison between analytic results and LS-DYNA simulation results for various masses (2 kg~9 kg) of lattice structure. As seen in Fig. 17, the values of the total crash energy absorbed of the analytic model and the FEM model for the lattice structure are in good agreement. The results obtained from the modified analytic model of this paper are much better than the results obtained in the previous paper (Lee *et al.* 2007). Note that the semi-empirical formulation yields less energy absorption with respect to LS-DYNA predictions in most cases. This is because the semi-empirical formulations ignored some local buckling effects and the self-contact effects between the thin-walled members.
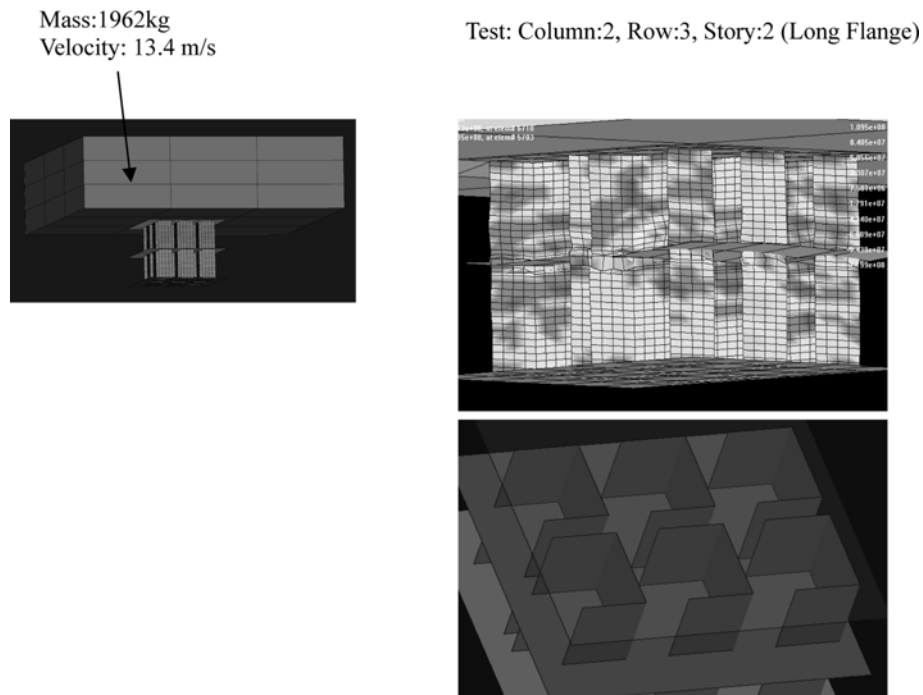

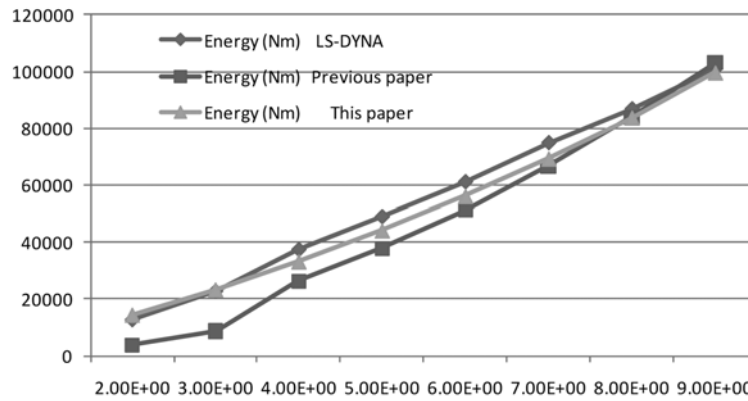Fig. 16 FEM model for verification of analytic solution

Fig. 17 Absorbed energy of analytic model and LS-DYNA simulation (X axis: mass of lattice structure (kg), Y axis: energy (Nm))

Table 1 Absorbed energy of analytic model and LS-DYNA simulation

Mass (kg)	Energy (Nm) LS-DYNA	Energy (Nm) Previous paper	Energy (Nm) This paper
2.00E+00	12910	3902	14537
3.00E+00	22930	8776	23405
4.00E+00	37530	26411	33266
5.00E+00	49030	37869	44152
6.00E+00	61120	51279	56119
7.00E+00	74810	66610	69250
8.00E+00	86696	83890	83665
9.00E+00	100773	103120	99524

Note that in this research, the number of lobes, and the elongation factor $\alpha_{lattice}$ and $\beta_{lattice}$ were obtained by using a finite element simulation. From the current simulation, 0.005 was used for $\alpha_{lattice}$ and $\beta_{lattice}$. For this method to be faster and more economical, these values should be determined by an analytic expression. These will be researched in the future.

5. Conclusions

The objective of this paper is to develop a reconfigurable lattice structure for the improved crashworthiness of vehicles, and to develop an improved First Order Analysis model for predicting crash energy absorption of an expandable lattice structure. In ELS, an identical unit element is repeated in the directions of story, row, and column. To develop the modified analytic model, a stiffness approach for the elastic region and a modified plastic limit analysis with pure plastic bending deformation and amended elongation factors for plastic region were developed. The total absorbed energy obtained with the previous model, current model, and a full finite element model has been compared. It is seen that the modified model is in much better agreement with the full

finite element model.

Future research will consider the ELS being supported by the vehicle body and the strain rate effect as well as other possible deformation shapes of the thin-walled structural members in the ELS. Manufacturability, sensing technology and actuation mechanism will be further investigated for potential implementation of the new technology in innovative vehicle applications.

Acknowledgements

References

Aktay, L., Johnson, A.F. and Holzapfel, M. (2005), "Prediction of impact damage on sandwich composite panels", *Comput. Mater. Sci.*, **32**(3-4), 252-260.

Alghamdi, A. (2001), "Collapsible impact energy absorbers: an overview", *Thin Wall. Struct.*, **39**(2), 189-213.

Avalle, M., Chiandussi, G. and Belingardi, G. (2002), "Design optimization by response surface methodology: application to crashworthiness design of vehicle structures", *Struct. Multidiscip. O.*, **24**(4), 325-332.

Crandall, S.H., Dahl, N.C. and Lardner, T.J. (1978), *An Introduction to The Mechanics of Solids*, McGraw-Hill.

Deb, A., Mahendrakumar, M.S., Chavan, C., Karve, J., Blankenburg, D. and Storen, S. (2004), "Design of an aluminium-based vehicle platform for front impact safety", *Int. J. Impact Eng.*, **30**(8-9), 1055-1079.

Han, J. and Yamazaki, K. (2003), "Crashworthiness optimization of s-shape square tubes", *Int. J. Vehicle Des.*, **31**(1), 72-85.

Hibbeler, R.C. (2005), *Mechanics of Materials*, Pearson/Prentice Hall.

Kawamura, H., Ohmori, H. and Kito, N. (2002), "Truss topology optimization by a modified genetic algorithm", *Struct. Multidiscip. O.*, **23**, 467-472.

Kim, H.S. and Wierzbicki, T. (2001), "Effect of the cross-sectional shape on crash behaviour of a three dimensional space frame", *Int. J. Vehicle Des.*, **25**(4), 295-316.

Lee, D.W., Ma, Z.D. and Kikuchi, N. (2007), "Analytic model of a crash energy absorption structure for crashworthy design of an inflatable morphing body", *Proceedings of the ASME IMECE*, Seattle, November.

Lee, D.W., Ma, Z.D. and Kikuchi, N. (2008), "An innovative I-bumper concept for improved crashworthiness of military and commercial vehicles", SAE 2008 World Congress, SAE Technical Paper Number 2008-01-0512.

Lingyun W., Mei, Z., Guangming, W. and Guang, M. (2005), "Truss optimization on shape and sizing with frequency constraints based on genetic algorithm", *Comput. Mech.*, **35**, 361-368.

Malen, D. and Kikuchi, N. (2006), *Course Pack of ME513: Auto Body Structure*, University of Michigan.

Pedersen, N.L. and Nielsen, A.K. (2003), "Optimization of practical trusses with constraints on eigenfrequencies, displacement, stresses, and buckling", *Struct. Multidiscip. O.*, **25**, 436-445.

Pedersen, C.B.W. (2004), "Crashworthiness design of transient frame structures using topology optimization", *Comput. Meth. Appl. Mech. Eng.*, **193**, 653-678.

Rhodes, J. (2001), "Some observations on the post-buckling behaviour of thin plates and thin-walled members", *Proceedings of the Third International Conference on Thin-Walled Structures*, Cracow, Poland, June.

Schafer, B.W. (2002), "Local, distortional, and euler buckling of thin-walled columns", *J. Struct. Eng.*, **128**(3), 289-299.

Sedaghati, R., Suleman A. and Tabarrok, B. (2001), "Optimum design of adaptive truss structures using the integrated force method", *Proceedings of the 42nd AIAA/ASME/ASCE/AHS/ASC Structures, Structural*

Dynamics, and Materials Conference and Exhibit, **2**(2), 259-271.

Suh, M.W., Lee, J.H., Cho, K.Y. and Kim, S.I. (2002), "Section property method and section shape method for the optimum design of vehicle body structures", *Int. J. Vehicle Des.*, **30**(1-2), 115-134.

Yasui, Y. (2000), "Dynamic axial crushing of multi-layer honeycomb panels and impact tensile behavior of the component members", *Int. J. Impact Eng.*, **24**(6-7), 659-671.

Yu, W.W. (2000), *Cold-Formed Steel Design*, John Wiley and Sons.